



# DESY Summer student program

## The effective W approximation

Thomas Veness  
 St Anne's College, University of Oxford  
 Supervised by Jürgen Reuter, DESY Theory Group

September 5, 2012

### Abstract

We investigate the effective W approximation (EWA) and its implementation in WHIZARD [1]. We follow the derivation of the EWA as presented in [2] and consider some of the limitations on its validity as discussed in [3, 4]. We attempt to verify the code in WHIZARD and analyse data from the software to validate the implementation. We find that although the implementation appears to be valid, that there are some concerning results both inherently with the EWA and also with the magnitude of the deviations of the extracted structure function from the analytical structure function.

## 1 Introduction

The main practical application of the effective W approximation is to reduce the process of evaluating cross sections of the form of figure 1, from a highly complicated process, to evaluating the cross section for smaller diagrams and integrating out the heavy bosons as a number density distribution which is a function of the momentum transfer  $x_i$  of the fermion carried away by the boson i.e. we wish to write our cross section in the form

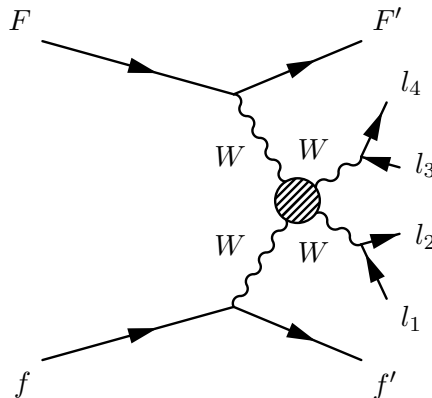


Figure 1: Example processes where the EWA is applicable

$$\sigma(Ff \rightarrow F'f'X) = \sum_{\text{pols } \lambda, \lambda'} \int_0^1 \int_0^1 dx_1 dx_2 \sigma(WW \rightarrow X | p_{W_1} = p_1 x_1, p_{W_2} = p_2 x_2) F_\lambda(x_1) F_{\lambda'}(x_2) \quad (1)$$

This is very similar to the idea of factorisation for parton distribution functions. This is much easier for software to handle, and is especially versatile when we have an analytical form for the distribution functions. The EWA also allows physical insight into a process; when it agrees well with a full calculation, it helps us to understand the physics of the process in question. The  $F_\lambda(x_i)$  represent number density functions for a  $\lambda$ -polarised  $W^\pm$  being radiated by a fermion with momentum fraction  $x_i$  — entirely akin to the Weizsäcker-Williams effective photon approximation (EPA) [5, 6, 7].

## 2 The effective W approximation

### 2.1 Matrix elements

We follow very closely an approach taken to exhibit the Weizsäcker-Williams method for the EPA in [8], in an equivalent treatment to [2, 9] to obtain the structure functions for the EWA. The major difference when compared to the EPA is that, as the vector bosons being radiated are massive, we must also consider the physical longitudinal polarisation states.

We consider only the case where a (massless) fermion radiates the boson, but in principle it would also be possible to consider a massive fermion or even a different boson being radiated. The expression can be broken up and we need only consider the evaluation of the diagram in figure 2.

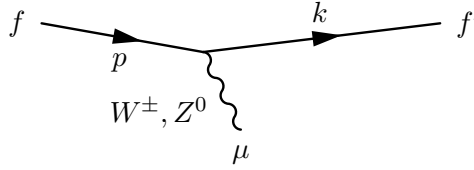


Figure 2: W/Z “splitting” process

We consider an on-shell fermion radiating a boson approximately collinearly at a high centre-of-mass-energy (such that we can neglect the fermion mass term). If the boson is not emitted exactly collinearly, then it must be off-shell. The crux of the approximation is that we make the assumption that the boson is close enough to being on-shell that, in the amplitude of the sub-process in which it is later involved, we can take it to be on-shell. This means that the treatment will only necessarily be valid when  $\sqrt{s} \gg M_V$ , the mass of the vector boson. The 4-vectors are, if the boson carries away a momentum fraction  $x$ , to order  $p_\perp^2$  (the square of the perpendicular three-momentum of the off-shell boson):

$$p = \begin{pmatrix} p \\ 0 \\ 0 \\ p \end{pmatrix}, \quad k = \begin{pmatrix} (1-x)p \\ -p_\perp \\ 0 \\ (1-x)p + \frac{p_\perp^2}{2xp} \end{pmatrix}, \quad q = \begin{pmatrix} xp \\ p_\perp \\ 0 \\ xp - \frac{p_\perp^2}{2xp} \end{pmatrix} \quad (2)$$

The amplitude for the process, from the electroweak Feynman rules [10], is simply given by

$$i\mathcal{M} = -i\bar{u}(k)\not{\epsilon}^*(q)(g_V - g_A\gamma^5)u(p). \quad (3)$$

This can be cranked through relatively quickly by use of the trace theorems, but it is more instructive to obtain the individual structure functions for both the transverse and

Polarisation	$\mathcal{M}$ (Left handed fermion)	$\mathcal{M}$ (Right handed fermion)	Helicity average $ \mathcal{M} ^2$
Right handed	$p_\perp \frac{\sqrt{2(1-x)}}{x} (g_V + g_A)$	$p_\perp \frac{\sqrt{2(1-x)}}{x} (g_V - g_A)$	$p_\perp^2 \frac{2(1-x)}{x^2} (g_V^2 + g_A^2)$
Left handed	$\sqrt{2} \frac{p_\perp}{x\sqrt{1-x}} (g_V + g_A)$	$\sqrt{2} \frac{p_\perp}{x\sqrt{1-x}} (g_V - g_A)$	$p_\perp^2 \frac{2}{x^2(1-x)} (g_V^2 + g_A^2)$
Left handed	$2p\sqrt{1-x} \frac{m_V}{xp} (g_V + g_A)$	$2p\sqrt{1-x} \frac{m_V}{xp} (g_V - g_A)$	$\frac{4m_V^2(1-x)}{x^2} (g_V^2 + g_A^2)$

Table 1: Summary of the matrix elements for the EWA

the longitudinal polarisations. If we initially consider a left-handed electron, the spinors are approximately given by

$$u(k) = \begin{pmatrix} \frac{p_\perp}{2(1-x)p} \\ 1 \\ 0 \\ 0 \end{pmatrix}, \quad u(p) = \begin{pmatrix} 0 \\ 1 \\ 0 \\ 0 \end{pmatrix}. \quad (4)$$

Working in the helicity basis, we have that in  $2 \times 2$  block form:

$$\gamma_\mu = \begin{pmatrix} 0 & \sigma_\mu \\ \bar{\sigma}_\mu & 0 \end{pmatrix}, \quad \gamma^5 = \begin{pmatrix} -1 & 0 \\ 0 & 1 \end{pmatrix}. \quad (5)$$

We also choose our polarisation basis similarly to [9]; making the approximation that  $k_0 \gg M_V$  and choosing positive and negative helicity transverse polarisation vectors.

$$\begin{aligned} \epsilon_0 &= \frac{i}{M_V} (q_0, 0, 0, |\mathbf{q}|) \\ \epsilon_1 &= \frac{1}{\sqrt{2}} \left( 0, 1, i, -\frac{p_\perp}{px} \right) \\ \epsilon_2 &= \frac{1}{\sqrt{2}} \left( 0, 1, -i, -\frac{p_\perp}{px} \right) \\ \epsilon_3 &\approx \frac{M_V}{2k_0} (-1, 0, 0, 1) \end{aligned} \quad (6)$$

We can now evaluate the amplitudes for the various processes for a left-handed electron. For the right-handed electron, the only change is that  $g_A \rightarrow -g_A$  due to the pseudoscalar nature of  $\gamma^5$ . The results for the various amplitudes are presented in table 1.

## 2.2 From matrix elements to distribution functions

If we make the (bold) assumption that the process involving the exchanged bosons doesn't depend on the polarisation, then we are justified in considering the unpolarised cross section. Thus, using the same notation as in figure 2, we have that, as in the EPA derivation in [8], the cross section is given by

$$\sigma = \frac{1}{(1+v_X)2p2E_X} \int \frac{d^3k}{(2\pi)^3} \frac{1}{2k^0} \int d\Pi_Y \langle |\mathcal{M}|^2 \rangle \left( \frac{1}{q^2} \right)^2 |\mathcal{M}_{VX}|^2, \quad (7)$$

where  $\int d\Pi_Y$  denotes integrating over the phase space of  $Y$ , and  $v_X$  is the velocity of the (potentially composite) particle  $X$ . Substituting for  $k^0$  and  $q^2$  from our earlier definitions in equation 2, we obtain that

$$\sigma = \int \frac{dx dp_\perp^2}{16\pi^2} \frac{x(1-x)}{p_\perp^4} \langle |\mathcal{M}|^2 \rangle \sigma(VX \rightarrow Y). \quad (8)$$

We finally have the total cross section for the process to be of the form of equation 9, we can therefore identify the number density distribution we are looking for as shown in equation 10.

$$\sigma_{\text{total}}(fX \rightarrow f'Y|k, p, k', p') = \sum_{\lambda} \int_0^1 F_{\lambda} \sigma(W^{\pm}, Z^0|xp, k, k') dx \quad (9)$$

$$F_{\lambda} = \int \frac{dp_{\perp}^2}{p_{\perp}^4} \langle |\mathcal{M}_{\lambda}|^2 \rangle \frac{x(1-x)}{16\pi^2} \quad (10)$$

We integrate between the limits from  $\bar{x}M_V^2$  (where  $\bar{x} = 1 - x$ ) up to  $p_{\perp\text{max}}^2 + \bar{x}M_V^2$ , where we drop writing the “max” from now on. A summary for the different distribution functions can be found in table 2, where we have used the values of  $g_V$  and  $g_A$  appropriate to the vector bosons. As can be seen by inspection, if we take the average of the two transverse modes, we obtain exactly the same answer as in [2]<sup>1</sup>.

Particle	$F_0(x)$	$F_+(x)$	$F_-(x)$
$W^{\pm}$	$\frac{\bar{x}}{4\pi^2 x} \frac{p_{\perp}^2}{\bar{x}m_W^2 + p_{\perp}^2} (g_V^2 + g_A^2)$	$\frac{\bar{x}^2}{8\pi^2 x} \ln \left( \frac{p_{\perp}^2 + \bar{x}m_W^2}{\bar{x}m_W^2} \right) (g_V^2 + g_A^2)$	$\frac{1}{8\pi^2 x} \ln \left( \frac{p_{\perp}^2 + \bar{x}m_W^2}{\bar{x}m_W^2} \right) (g_V^2 + g_A^2)$
$Z^0$	$\frac{\bar{x}}{4\pi^2 x} \frac{p_{\perp}^2}{\bar{x}m_Z^2 + p_{\perp}^2} (g_V^2 + g_A^2)$	$\frac{\bar{x}^2}{8\pi^2 x} \ln \left( \frac{p_{\perp}^2 + \bar{x}m_Z^2}{\bar{x}m_Z^2} \right) (g_V^2 + g_A^2)$	$\frac{1}{8\pi^2 x} \ln \left( \frac{p_{\perp}^2 + \bar{x}m_Z^2}{\bar{x}m_Z^2} \right) (g_V^2 + g_A^2)$

Table 2: Summary of the effective W/Z approximation distribution functions

### 2.3 Calculating a cross section by hand

Using the results from [2], we check that the EWA can indeed produce an accurate cross section for a simple process. A process that it should be able to replicate very well is vector boson fusion to produce a Higgs boson, as figure 4 should be the only diagram contributing to the process. This calculation also exploits the fact that the longitudinally polarised boson mode dominates over the transverse modes at high energies, simplifying the calculation even more. The result is given in equation 11. Inserting the Higgs value implemented in WHIZARD and examining various values of  $\sqrt{s}$ , we obtain the results shown in table 3. It is quite clear from this table that the results of the EWA become steadily more accurate at higher energies, which is what we expect, as at higher energies we can more legitimately treat the intermediate boson as being on-shell and decouple it from the rest of the process. If we go to steadily higher energies, the process becomes numerically unstable and takes a long time to converge — this is shown in figure 3. If the process is run with considerably more iterations, then this bad behaviour goes away, but it is a practical issue to be aware of when performing a calculation that may seem to be giving nonsense.

$\sqrt{s}$ (GeV)	$\sigma_{\text{EWA}}$ (fb)	$\sigma_{\text{WHIZARD}}$ (fb)	Ratio
500	65.57	34.07	1.9
1000	210.0	147.2	1.4
2000	329.9	313.8	1.3
5000	654.7	566.9	1.2
10000	976.2	886.5	1.1
15000	1330	1219	1.09
50000	1534	1447	1.06

Table 3: Various cross sections for Higgs production via vector boson fusion

<sup>1</sup>We say “exactly the same answer”, but actually we believe there is a small mistakes in [2], where in one of the explicit structure functions, they have written  $\sin^2 \theta_W^2$  instead of  $\sin^2 \theta_W$ . Apart from this, we completely agree with their results.

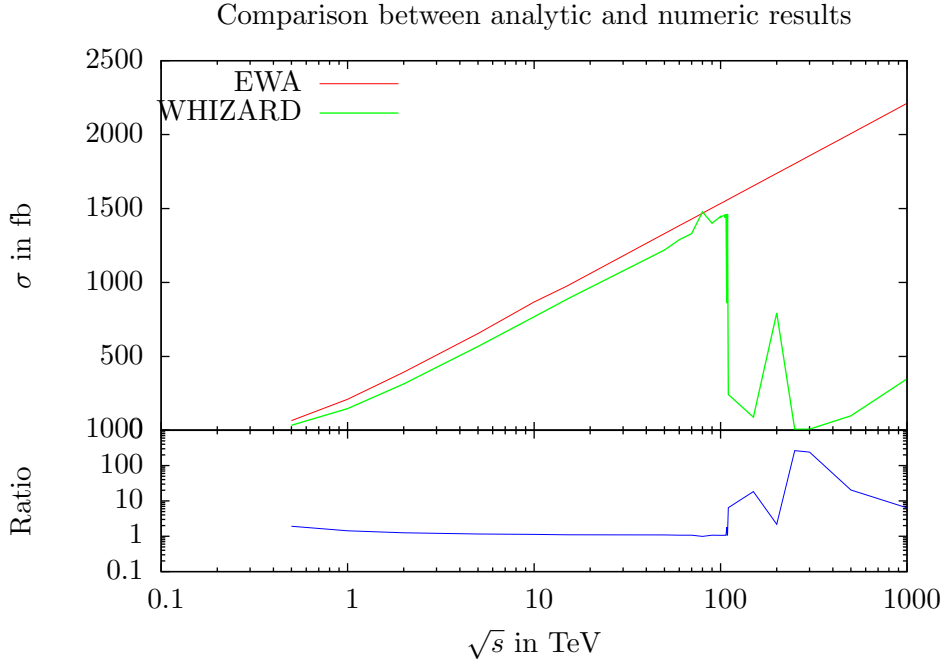


Figure 3: A graph of the values predicted from the analytic expression compared against WHIZARD. It can be seen that at extremely high energies ( $\sqrt{s} \sim 100$  TeV) that the numerical method becomes unstable at this number of iterations and events simulations (12:100000,5000). The top section shows the cross sections predicted by both, whilst the bottom shows the ratio  $\sigma_{\text{EWA}}/\sigma_{\text{WHIZARD}}$ .

$$\sigma(e^- \mu^+ \rightarrow \nu_e \bar{\nu}_\mu H) = \frac{g^2}{64\pi m_W^2} \left[ \left(1 + \frac{m_H^2}{s}\right) \ln\left(\frac{s}{m_H^2}\right) + 2 \left(\frac{m_H^2}{s} - 1\right) \right] \quad (11)$$

## 2.4 Regimes of validity of the EWA

The point originally raised in [11] is that we can't simply neglect diagrams on physical grounds — assigning individual diagrams a physical meaning is a classic case of the mind-project fallacy: diagrams are merely a calculational convenience rather than a physical process: it is only when summed together that they begin to mean something. This is because the choice of gauge is arbitrary, so different diagrams can give different answers: by throwing away diagrams, we break gauge invariance, which is something that should never be taken lightly. A particular choice of gauge (the axial gauge) is made in [3, 4] and calculations justifying the EWA are performed.

The main conditions for validity are that the energy scale of the hard scattering process is much larger compared to the virtuality of the boson. When this is true, all small virtualities may be ignored and thus the boson may be treated as approximately on-shell (as is required to make sense of combining it with the cross section which has an on-shell inbound boson). The key to establishing a large enough hard interaction energy scale is by having the transverse momentum of the radiated boson being relatively large compared to  $m_V$ .

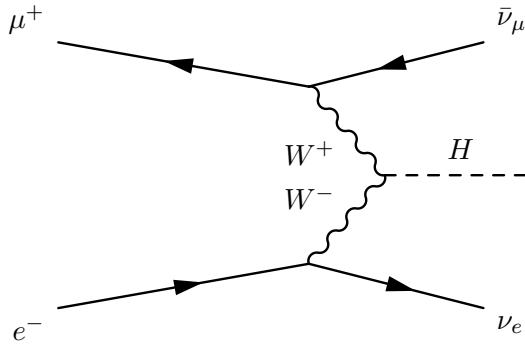


Figure 4: Simple diagram for comparing the EWA cross section and a fully simulated cross section

### 3 Verifying the implementation

#### 3.1 How it's implemented in WHIZARD

The basic idea, as covered before, is that we evaluate the cross section for a specific sub-process and then fold this with the EWA distribution functions to find the cross section for the total process. We can immediately begin to spot some problems, here. A lot of the problems are in our assumptions and simply restrict us to certain kinematic regimes, such as being at a sufficiently high energy to ensure that the vector boson can be considered as on-shell. We also require that the sub-process does not depend on the polarisation of the vector boson in our implementation, otherwise we should evaluate something more like equation 12, where  $\sigma_\lambda$  is the cross section for the appropriate polarised process to occur. We have assumed throughout that the different polarisations do not interfere in any significant manner and continue to do so in the implementation of WHIZARD.

$$\sigma_{\text{total}}(fX \rightarrow f'Y|k, p, k', p') = \sum_\lambda \int_0^1 F_\lambda(x) \sigma_\lambda(W^\pm, Z|xp, k, k') dx \quad (12)$$

The biggest problem, which also seems the most difficult to surmount, is that of background processes which can't be ignored. Consider the process  $\nu_e \bar{\nu}_e \rightarrow e^- e^+ W^- W^+$ . When we start to draw out the diagrams, we might consider the class of diagrams as shown in figure 5(a), for which the EWA can be applied perfectly well. We might be tempted, in the axial gauge, to apply the EWA to the entire process, but doing so would not yield a useful result, as significant contributions to the *amplitude* come from diagrams of the form as shown in 5(b), which cannot be treated with the EWA and thus cause our estimate of the cross section to be incorrect by orders of magnitude.

WHIZARD implements the EWA relatively simply, defining the structure functions, remapping the unit interval to attempt to avoid the  $1/x$  singular behaviour for numerical stability reasons and then integrating over the structure functions with the cross section of the sub-process. The main issue we face is what our choice of the cut-off on  $x$  should be, as by choosing  $x_{\min}$  to be small, we can potentially make the cross section to be evaluated arbitrarily large, which is clearly false. For reasons purely of convenience and that they seem to give answers that are not too large, we conventionally choose  $x_{\min} = 0.1$ . We now seek to verify that the implementation has indeed been performed correctly in WHIZARD — we ideally seek a process from which we can extract the structure function numerically and then compare it against the analytic result. We would wish to choose a process which we can simulate fully without the EWA and also extract a structure function from that, but so far this has proved to be difficult.

#### 3.2 The code in WHIZARD

We can verify that the code in WHIZARD indeed reflects the EWA as we have derived it. It should be noted that the code in WHIZARD goes to a higher order than we have done, but

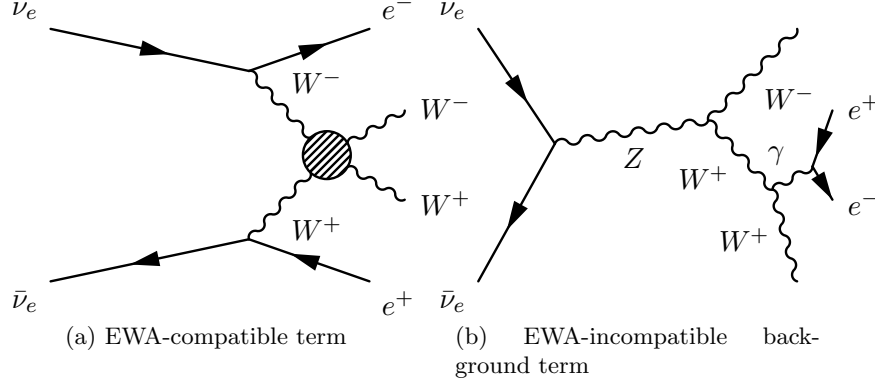


Figure 5: An example of a process ( $\nu_e \bar{\nu}_e \rightarrow e^- e^+ W^- W^+$ ) for which some terms are compatible with the EWA, yet significantly contributing background terms cause the treatment to be potentially invalid

to leading order, the results agree (and at high energies, the NLO term becomes negligible — the high-energy regime is also the regime of greatest validity for the EWA, anyway). As mentioned before, because of the  $1/x$  type behaviour, the unit interval is remapped to a new variable  $r$  such that our integration measure is given by equation 13, where the notation  $\bar{r} = (1 - r)$  is used.

$$x = e^{\bar{r} \ln x_0 - r \ln x_1} \Rightarrow \int_{x_0}^{x_1} \frac{dx}{x} = (\ln x_1 - \ln x_0) \int_0^1 dr \quad (13)$$

Thus, when implemented in the code, it may appear that a factor of  $1/x$  is missing, but the code in fact integrates over  $r$  (and applies the factor of the difference of logarithms), so the integration measure should be correct. The relevant code sections for the  $Z$  from `sf_ewa.f90` are included in code block 1. The code for the  $W$  is identical in concept, except  $m_Z \rightarrow m_W$  and  $c_V = c_A = g/(2\sqrt{2})$ .

```
data%cv = g / 2._default
data%ca = g / 2._default
data%coeff = 1._default / (8._default * PI**2)
f = data%coeff * (lx1 - lx0)
c1 = log (1 + pt2 / (xb * (data%MZ)**2))
c2 = 1 / (1 + (xb * (data%MZ)**2) / pt2)
cv = data%cv * (t3 - 2._default * q * data%sinthw**2) / data%costhw
ca = data%ca * t3 / data%costhw
fm = ((cv + ca)**2 + ((cv - ca) * xb)**2) / 2 * (c1 - c2)
fp = ((cv - ca)**2 + ((cv + ca) * xb)**2) / 2 * (c1 - c2)
fL = (cv**2 + ca**2) * 2 * xb * c2
fsum = fp + fm + fL
f = f * fsum
```

We start by setting the values of  $c_V$  and  $c_A$  to a common factor  
Both functions have a pre-factor of  $1/(8\pi^2)$   
We start  $f$  off with the pre-factor and include the integration measure factor  
 $c_1$  and  $c_2$  are the two different functions found multiplying the whole expressions

We account for the fact that  $Z$ -boson coupling depends on particle properties  
The structure functions: note that they have a different form to the ones we derived,  
we believe that this is because a different helicity basis has been used.  
As we sum all of them together, it doesn't make a difference to the final results.  
We finally sum them together and bring all of the factors together

Code block 1: The relevant section of the WHIZARD code for implementing the structure function(s) of the EWA

### 3.3 Extracting the structure function

The aim here is to run a process using the EWA and then recover the structure function from data from the process — this is useful as if we can recover the structure function via the expected method, then it should be implemented correctly. That is, if we make a generic procedure to find an “effective structure function” for a sub-process and for the EWA sub-process it produces the EWA structure function, then WHIZARD almost definitely has a correct implementation *up to a scaling factor*. The idea is to find the number of events for a given momentum fraction transfer: this should be proportional to the term

$$\sum_{\lambda} F_{\lambda}(x) \sigma_{\text{sub}} \Delta x.$$

However, we can further simplify this as WHIZARD allows us to override the matrix element for the sub-process and manually set it to a constant which, in the absence of a structure function, would integrate to 1 fb. This means that the sub-process in question doesn't (in principle) matter. In this case, with constant-width bins, the number of events in a bin is just proportional to the structure function. To within a linear scaling factor of the whole graph, we should be able to recover the EWA structure function. So, considering the process  $e^- \mu^- \rightarrow e^- \mu^- Z$ , we can see that the only diagrams contributing to this process at tree level within the EWA are shown in figure 6. Because we are at a high centre of mass energy, we are justified in taking the leptons to be massless. This means that the initial electron energy  $E_e = \frac{\sqrt{s}}{2}$  and the final electron energy will be denoted by  $E'_e$ . The momentum fraction is therefore given by  $1 - x = \frac{E'_e}{E_e} = \frac{2E'_e}{\sqrt{s}}$ . When we use WHIZARD to record these values and then scale the structure function, we obtain the graph shown in figure 7. The structure function has been scaled by an arbitrary factor, as we can only check the functional form by this method, as we necessarily produce what is effectively a properly normalised probability distribution, as the number of events is fixed.

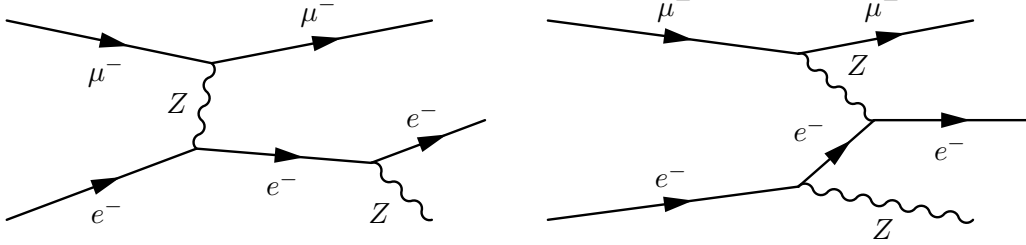


Figure 6: EWA diagrams contributing to the process  $e^- \mu^- \rightarrow e^- \mu^- Z$

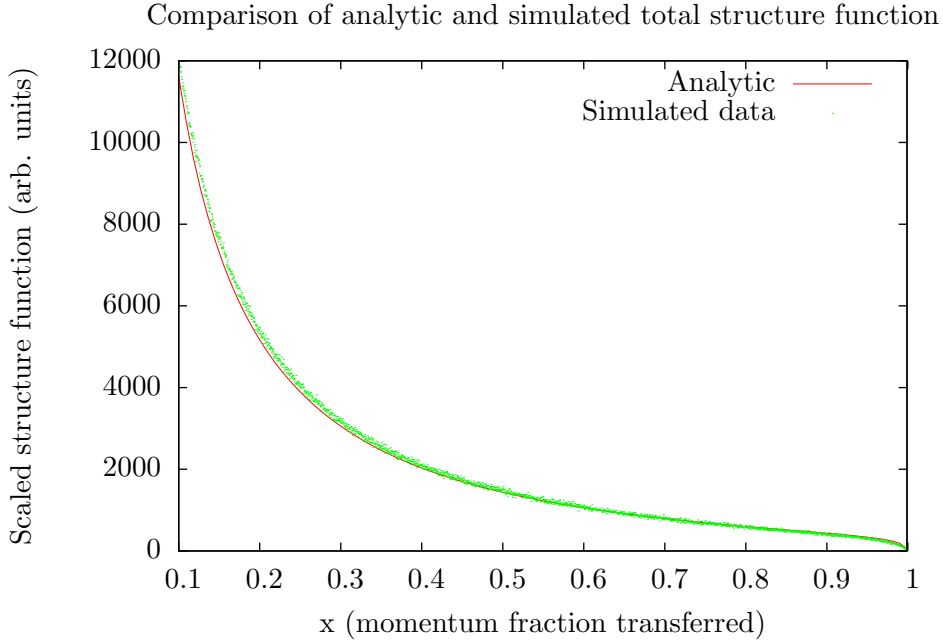


Figure 7: A plot of the extracted strucutre function compared with the analytic structure function

The fit looks pretty good, but we can appreciate the goodness of the fit by examining



the percentage difference between the extracted structure function and the analytic function as shown in figure 8.

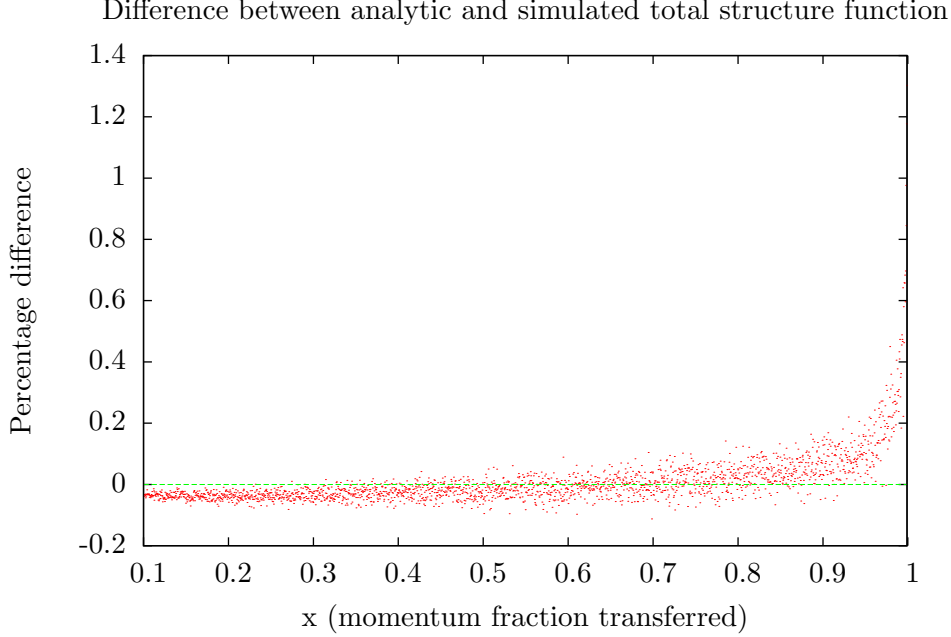


Figure 8: A plot of the percentage different between the extracted structure function and the analytic structure function for the EWA.

We can see that the structure function seems to be slightly too small for small  $x$  and the fractional error gets very large for  $x$  near 1. These are two areas of the graph where the gradient gets very large, so there may be numerical stability issues caused by this. To see if there is some sort of systematic effect on the errors, we modify the source code of WHIZARD to have a constant structure function. The fractional errors for this are shown in figure 9. As can be seen, the errors appear to be uniformly random, but the magnitude of the errors is still a little concerning; the reason for such large deviations is still unknown.

### 3.3.1 Checking the overall factor

The overall factor in front of the structure function *can*, however, be checked by evaluating cross sections. In principle, we can also check that we have the correct functional form this way, too but it is more a trial by exhaustion (and does not guarantee uniqueness in finite time!) rather than the more elegant method of actually extracting the function. The simplest way to test the cross sections is by forcing the hard process to have a cross section of 1fb (again), independent of the other details of the process. We can then check our result against processes which both 1 and 2 radiated bosons. We should also check that WHIZARD is indeed implementing this restriction on the sub-process correctly — something we should check is that the cross section is the same independent of the details of the hard interaction. The corresponding calculation can then be performed outside of WHIZARD using a numerical integration package [12]. We will, in general, look at a process of the form  $e^\pm \mu^\pm \rightarrow W/Z W/Z + \dots$ , depending on what combination of structure functions we are intending to test.

To ensure thought in our numerical calculations we didn't miss out any small factors by hand in front of the structure function, we change the source code of WHIZARD to make the structure function very simple. If we can't, for example, agree on the magnitude of a constant structure function, then for the full structure function any problems will be more difficult to diagnose. For this simple process we expect the cross section for a one-particle

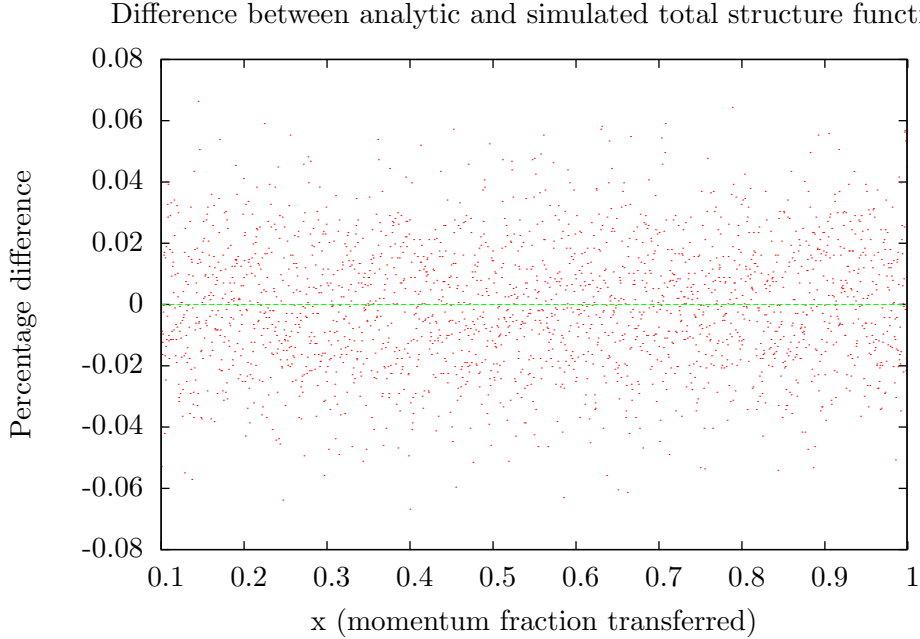


Figure 9: A plot of the percentage difference between the extracted structure function and the analytic structure function for a constant function.

and two-particle process to be given by equations 17 and 18 respectively. We also note that the structure function for the  $Z$  boson is simply larger (once changing the  $m_W$  for and  $m_Z$ , which typically makes little difference) by a factor of  $((T_3^f - 2Q^f \sin^2 \theta_W)^2 + (T_3^f)^2)$ , which we denote by  $\eta_Z$ . We also denote  $\int_{x_{\min}}^1 \sum_{\lambda} F_{\lambda}^{W^{\pm}} dx$  by  $I(x_{\min})$  and the corresponding integral for  $Z$  bosons by  $\eta_Z I_Z(x_{\min})$ , we also drop the explicit  $x_{\min}$  dependence, but  $I$  is indeed still a function of  $x_{\min}$ . Hence, we can express all of the cross sections for the one-particle processes and calculate them numerically in table 4. We can then take the values of the cross sections from WHIZARD and take the ratio of the two to compare how well they fit. A plot of this is shown in figure 10. As can clearly be seen from the plot, WHIZARD introduces a factor of 1.5 for each of the single-EWA emissions and thus a factor of 2.25 is introduced for a double-EWA process — there is evidently some sort of systematic effect going on here. To be sure that it was not a mistake in the implementation of the structure functions on either end, the code in WHIZARD was changed to have a structure function equal to various functions: unity;  $x$ ;  $x^2$ ;  $\ln x$ , and these were equally incorrect by a factor of 1.5. This merited further investigation and reasoning to try to figure out the cause of this and whether it manifests itself in cross section calculations for more realistic processes or whether it is merely an artefact of using the test matrix element.

The solution to this problem comes in recognising that there are mistakes in the definition of the “test matrix element” with regards to combinatorical factor of summing and averaging over the spins of the particles. The test matrix element has indices for helicities, colours and flavours. If we consider a process involving only different leptons as the incoming particles, then the colour and flavour indices are not summed over, as there is no degeneracy in this regard. The only thing remaining is helicity. If we consider the process  $e^- \mu^- \rightarrow e^- \mu^- Z$ , then to obtain a cross section for the process of 1 fb, the matrix element is defined as

$$\mathcal{M}(\text{hel}) = \text{const.} \quad (14)$$

for all of the helicity states. This means that if we sum over all of the helicities of the outbound state, we obtain  $\sum |\mathcal{M}|^2 = Na^2$ , where  $N$  is the number of helicities in the outbound state. We now need to account for averaging over the inbound states. Thus, we

	$W^+$	$W^-$	$Z$	$W^+W^-$	$W^+Z$	$W^-Z$	$ZZ$
Analytic $\sigma$	$I_W$	$I_W$	$\eta_Z I_Z$	$I_W^2$	$\eta_Z I_W I_Z$	$\eta_Z I_W I_Z$	$\eta_Z^2 I_Z^2$
$x_{\min} = 0.1$	$2.749 \times 10^{-2}$	$2.749 \times 10^{-2}$	$8.584 \times 10^{-3}$	$7.558 \times 10^{-4}$	$2.360 \times 10^{-4}$	$2.360 \times 10^{-4}$	$7.369 \times 10^{-5}$
$x_{\min} = 0.2$	$1.661 \times 10^{-2}$	$1.661 \times 10^{-2}$	$5.177 \times 10^{-3}$	$2.760 \times 10^{-4}$	$8.601 \times 10^{-5}$	$8.601 \times 10^{-5}$	$2.680 \times 10^{-5}$
$x_{\min} = 0.3$	$1.099 \times 10^{-2}$	$1.099 \times 10^{-2}$	$3.416 \times 10^{-3}$	$1.207 \times 10^{-4}$	$3.753 \times 10^{-5}$	$3.753 \times 10^{-5}$	$1.167 \times 10^{-5}$
$x_{\min} = 0.4$	$7.462 \times 10^{-3}$	$7.462 \times 10^{-3}$	$2.314 \times 10^{-3}$	$5.569 \times 10^{-5}$	$1.727 \times 10^{-5}$	$1.727 \times 10^{-5}$	$5.354 \times 10^{-6}$
$x_{\min} = 0.5$	$5.053 \times 10^{-3}$	$5.053 \times 10^{-3}$	$1.562 \times 10^{-3}$	$2.553 \times 10^{-5}$	$7.891 \times 10^{-6}$	$7.891 \times 10^{-6}$	$2.439 \times 10^{-6}$
$x_{\min} = 0.6$	$3.324 \times 10^{-3}$	$3.324 \times 10^{-3}$	$1.023 \times 10^{-3}$	$1.105 \times 10^{-5}$	$3.401 \times 10^{-6}$	$3.401 \times 10^{-6}$	$1.047 \times 10^{-6}$
$x_{\min} = 0.7$	$2.048 \times 10^{-3}$	$2.048 \times 10^{-3}$	$6.210 \times 10^{-4}$	$4.193 \times 10^{-6}$	$1.284 \times 10^{-6}$	$1.284 \times 10^{-6}$	$3.931 \times 10^{-7}$
$x_{\min} = 0.8$	$1.095 \times 10^{-3}$	$1.095 \times 10^{-3}$	$3.326 \times 10^{-4}$	$1.200 \times 10^{-6}$	$3.644 \times 10^{-7}$	$3.644 \times 10^{-7}$	$1.107 \times 10^{-7}$
$x_{\min} = 0.9$	$3.997 \times 10^{-4}$	$3.997 \times 10^{-4}$	$1.194 \times 10^{-4}$	$1.598 \times 10^{-7}$	$4.774 \times 10^{-8}$	$4.774 \times 10^{-8}$	$1.426 \times 10^{-8}$

Table 4: The values of the form factors for various EWA processes

define out matrix element as

$$\mathcal{M} = \sqrt{\frac{\#_{\text{hel in}}}{\#_{\text{hel out}}}} \sqrt{\frac{\text{flux}}{\text{phase space volume}}} 1 \text{ fb} \quad (15)$$

This is then summed over all of the inbound states to complete the average. For the case of  $e^- \mu^- \rightarrow e^- \mu^- Z$ , we obtain the following overall factors for inbound states

$$\underbrace{\frac{1}{4}}_{\text{inbound fermion average}} \underbrace{(2 \cdot 3)}_{e^- Z} \underbrace{(2 \cdot 3)}_{\text{in } e^- Z} \underbrace{\left(\frac{1}{\sqrt{6}}\right)^2}_{\text{averaging of } e^- Z} = \frac{3}{2}, \quad (16)$$

which is exactly the factor we obtain! This calculation can be repeated for double boson emission and  $\frac{9}{4}$  is indeed recovered.

$$\sigma = \int_{x_{\min}}^1 \sum_{\lambda} F_{\lambda}^{W^{\pm}/Z}(x) dx \times 1 \text{ fb} \quad (17)$$

$$\sigma = \int_{x_{1\min}}^1 \int_{x_{2\min}}^1 \sum_{\lambda, \lambda'} F_{\lambda}^{W^{\pm}/Z}(x_1) F_{\lambda'}^{W^{\pm}/Z}(x_2) dx_1 dx_2 \times 1 \text{ fb} \quad (18)$$

### 3.4 Comparing WHIZARD against itself

An ideal way to check both the consistency and the accuracy of the EWA would be to compare a result from an EWA process with the result from a full process. A natural candidate for this would be the process examined before:  $e^- \mu^+ \rightarrow \nu_e \bar{\nu}_\mu H$ , but WHIZARD can't handle processes with a single-particle final state — which is what has to be resolved in the EWA sub-process  $W^+ W^- \rightarrow H$ . We are thus forced to consider a  $2 \rightarrow 2$  sub-process. To our knowledge, all of these involve more than one diagram *and* some of the diagrams are not accounted for by the EWA — this was one of our big concerns earlier.

The natural way to try to solve this problem is to apply cuts to the process. By applying appropriate cuts on, for example, the transverse momenta of the radiating fermions, we expect to reduce the overall process to a region in the parameter space where the EWA is the major contributor. In this way, we expect to be able to compare the EWA with the full process and comment on its validity, accuracy and usefulness.

So, what observables shall we investigate with respect to changing the cuts? The cross section is not ideal, as any local spikes can cause a large disagreement i.e. if the EWA causes a large disagreement at one point in  $\frac{d\sigma}{dx_1}$ , then if we examine this distribution, we can see that it might agree well in other areas, meanwhile just looking at  $\sigma$  doesn't tell us as much. As our main intuition about the validity of the EWA is related to the kinematic variable

Comparison of prediction from WHIZARD and calculation by hand

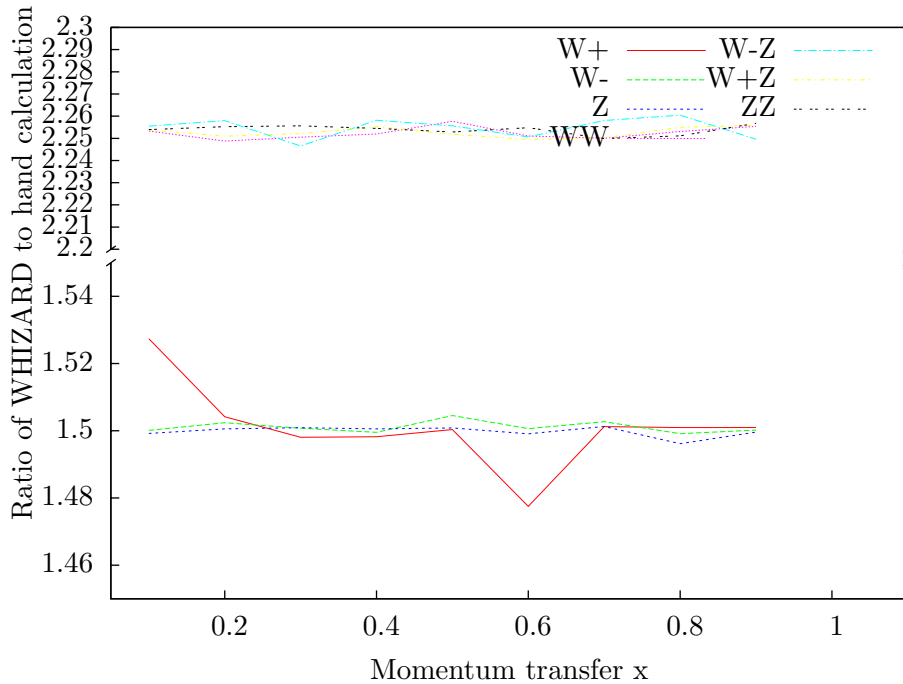


Figure 10: This shows the ratio  $\sigma_{\text{WHIZARD-EWA}}/\sigma_{\text{By-hand-EWA}}$ . The three single-bosons emissions all group together with a common factor of 1.5, whilst the four double-boson emissions group around 2.25 i.e.  $(1.5)^2$  — this clearly indicates that a factor of 1.5 is associated with the emission of each individual boson.

of the  $W$  bosons, we choose to investigate the energy distribution of one of the  $W$  bosons, applying cuts on the transverse momentum. Figure 11 shows the various distributions for associated applied cuts. We can see that the best agreement occurs when the energy of the  $W$  is higher — this makes sense, as we make the assumption that the energy of the interaction should be much larger than  $m_W$ . Also, the  $p_\perp$  cuts are most effective when the region is small i.e. in the regime where the assumption of  $p_\perp \ll E$  is valid. Both of the necessary conditions for the approximation to hold indeed seem to apply here.

## 4 Conclusions

We can see that clearly the basic structure of the implementation is valid. However, the random fluctuations exhibited in figures 8 and 9 are cause for concern. We have identified that the implementation of the test matrix element is responsible for the deviation of the magnitude of the expected structure function from the analytical results. Within this constant factor, the theory and data agree very well. It is also apparent that the EWA produces results consistent with full calculations in cases such as Higgs production via vector boson fusion and also reproduces features of other processes, such as  $W^+W^-$  scattering, when appropriate cuts are applied. Reproducing the actual cross section is yet to be exhaustively investigated in such a case, and would prove to be interesting research in the future.

### Upper cuts on Pt, W+ energy distribution

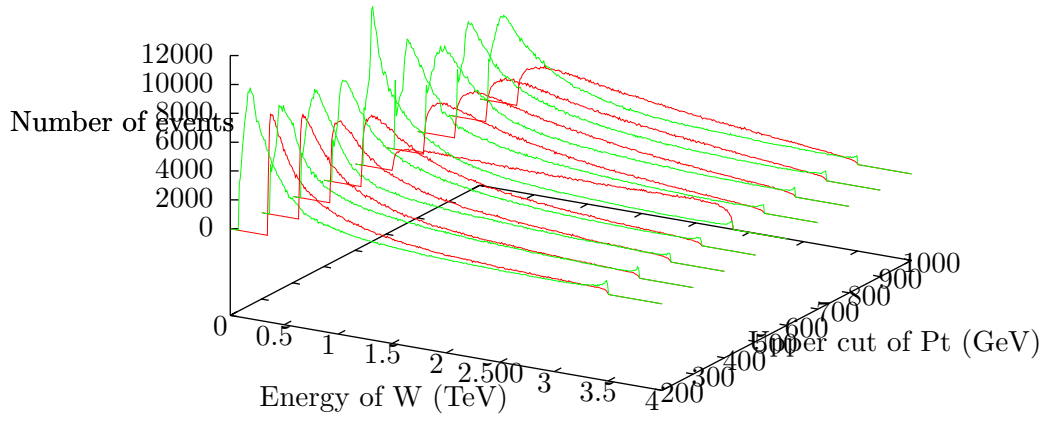


Figure 11: This shows the  $W$  energy distributions, with cuts of  $p_{\perp}$  above 100 GeV and below various different upper values

## References

- [1] Kilian, W., Ohl, T. & Reuter, J. WHIZARD: Simulating Multi-Particle Processes at LHC and ILC. *Eur.Phys.J.* **C71**, 1742 (2011). [0708.4233](#).
- [2] Kane, G., Repko, W. & Rolnick, W. The effective  $w$ ,  $z0$  approximation for high energy collisions. *Physics Letters B* **148**, 367 – 372 (1984). URL <http://www.sciencedirect.com/science/article/pii/0370269384901059>.
- [3] Borel, P., Franceschini, R., Rattazzi, R. & Wulzer, A. Probing the Scattering of Equivalent Electroweak Bosons. *JHEP* **1206**, 122 (2012). [1202.1904](#).
- [4] Kunszt, Z. & Soper, D. E. On the validity of the effective  $w$  approximation. *Nuclear Physics B* **296**, 253 – 289 (1988). URL <http://www.sciencedirect.com/science/article/pii/0550321388906736>.
- [5] Fermi, E. ber die theorie des stoess zwischen atomen und elektrisch geladenen teilchen. *Zeitschrift fr Physik A Hadrons and Nuclei* **29**, 315–327 (1924). URL <http://dx.doi.org/10.1007/BF03184853>. 10.1007/BF03184853.
- [6] Weizscker, C. F. v. Ausstrahlung bei sten sehr schneller elektronen. *Zeitschrift fr Physik A Hadrons and Nuclei* **88**, 612–625 (1934). URL <http://dx.doi.org/10.1007/BF01333110>. 10.1007/BF01333110.
- [7] Williams, E. J. Nature of the high energy particles of penetrating radiation and status of ionization and radiation formulae. *Phys. Rev.* **45**, 729–730 (1934). URL <http://link.aps.org/doi/10.1103/PhysRev.45.729>.
- [8] Peskin, M. E. & Schroeder, D. V. *An Introduction To Quantum Field Theory (Frontiers in Physics)* (Westview Press, 1995).
- [9] Dawson, S. The effective  $w$  approximation. *Nuclear Physics B* **249**, 42 – 60 (1985). URL <http://www.sciencedirect.com/science/article/pii/0550321385900380>.
- [10] Böhm, M., Denner, A. & Joos, H. *Gauge Theories of the Strong and Electroweak Interaction* (Vieweg+Teubner Verlag, 2001).
- [11] Kleiss, R. & Stirling, W. Anomalous high-energy behaviour in boson fusion. *CERN-TH* **4451**, 86 (1986).
- [12] Stein, W. *et al.* *Sage Mathematics Software (Version 4.8)*. The Sage Development Team (2012). <http://www.sagemath.org>.